Biosensors and Bioelectronics 86 (2016) 542–547

Contents lists available at ScienceDirect

Biosensors and Bioelectronics

journal homepage: www.elsevier.com/locate/bios

A fluorometric biosensor based on functional Au/Ag nanoclusters for real-time monitoring of tyrosinase activity

Hang Ao [a,1], Zhaosheng Qian [a,1], Yuyu Zhu [a], Meizhi Zhao [a], Cong Tang [a], Yuanyuan Huang [a], Hui Feng [a,*], Aijun Wang [b,*]

[a] College of Chemistry and Life Science, Zhejiang Normal University, Jinhua, 321004 China
[b] College of Geography and Environmental Sciences, Zhejiang Normal University, Jinhua, 321004 China

ARTICLE INFO

Article history:
Received 13 May 2016
Received in revised form
14 July 2016
Accepted 15 July 2016
Available online 16 July 2016

Keywords:
Au/Ag nanoclusters
Tyrosinase activity
Fluorometric assay
Biosensor
Photoinduced electron transfer (PET)

ABSTRACT

Due to the vital role of tyrosinase in melanin biosynthesis and its function as an important biomarker for melanoma cancer, highly sensitive detection of its activity using biocompatible materials is in urgent demand. Herein we report a convenient and highly sensitive fluorometric biosensor for tyrosinase activity detection based on biocompatible dopamine-functionalized Au/Ag nanoclusters (Dopa-Au/Ag NCs). Dopamine with redox property was covalently linked to Au/Ag NCs surface and formed a Dopa-Au/Ag NCs bioconjugate with strong blue fluorescence. Dopamine is readily oxidized by molecular oxygen under the catalysis of tyrosinase. After dopamine is transformed to *o*-dopaquinone, an intraparticle photoinduced election transfer (PET) process occurs between Au/Ag NCs and *o*-dopaquinone moiety, leading to the fluorescence quenching of the Dopa-Au/Ag NCs bioconjugate. Thus, this biosensor was utilized for sensitive and selective detection of tyrosinase in terms of the relationship between fluorescence quenching efficiency and tyrosinase activity. This study discovers that Au/Ag NCs and dopaquinone can serve as a good electron acceptor and donor pair which results in an efficient intraparticle photoinduced electron transfer process, and also provides another alternative way for tyrosinase activity monitoring.

1. Introduction

Tyrosinase (TYR, EC 1.14.18.1) is a copper-containing enzyme, which plays a vital role in the process of melanin synthesis in living organisms. Tyrosinase activity/level has been affirmed to be an essential biomarker of melanoma cancer and also acts as an autoantigen and serves as a marker for vitiligo (Baharav et al., 1996). Two continuous oxidation reactions of monophenols catalyzed by tyrosinase have been identified: the hydroxylation of monophenol to *o*-diphenol is catalyzed by its monophenolase activity, and then diphenol can be oxidized to *o*-quinones by its diphenolase in the presence of oxygen (Seo et al., 2003). Recently, tyrosinase was reported to be highly relevant to many disorders, such as chronic migraine (D'Andrea et al., 2013), Parkinson disease (Li, 2006), and even cancer (Mahoney et al., 2007; Lieberman et al., 2005; Sharman et al., 2012). The in-depth investigation of tyrosinase is of great significance for related biological research and medical diagnosis. Therefore, the development of highly sensitive assays of tyrosinase is in urgent demand for both fundamental research and practical application.

In the past few years, scientists have developed several methods for the detection of tyrosinase activity. Colorimetic (Kong et al., 2011; Li et al., 2012; Park et al., 2003), electrochemical (Yildiz et al., 2008) and fluorometric approaches (Gill et al., 2006; Yan et al., 2012; Wang et al., 2013; Li et al., 2010; Feng et al., 2008; Zhu et al., 2015; Liu et al., 2013; Teng et al., 2015) were utilized to measure the activity/level of tyrosinase. Compared with the other methods, fluorometric assays show its superior performance. Due to its high sensitivity, fast analysis and nondestructive nature, fluorometric method is regarded as a more desirable approach to monitor tyrosinase activity/level in a real-time manner. Although some fluoromeric assays for tyrosinase based on molecular probes, inorganic semiconductor quantum dots, carbon quantum dots had been developed in recent years, each type has their own disadvantages. Tedious synthesis process, complicated separation and purification processes, and instability to light irradiation are inherent drawbacks of molecular probes (Gill et al., 2006; Yan et al., 2012; Wang et al., 2013; Li et al., 2010), while those methods based on inorganic semiconductor quantum dots are concerned about its potential toxicity of used QDs in biological systems (Gill et al., 2006; Zhu et al., 2015). Despite advance in the development of

* Corresponding authors.
E-mail addresses: fenghui@zjnu.cn (H. Feng), ajwang@zjnu.cn (A. Wang).
[1] H. Ao and Z. Qian contributed this work equally.

http://dx.doi.org/10.1016/j.bios.2016.07.051
0956-5663/

tyrosinase assay based on biocompatible noble nanoclusters (Liu et al., 2013; Teng et al., 2015) has been made recently, detection approaches to achieve accurately quantitative evaluation of tyrosinase activity are still scarce up to date, and novel fluorescent nanomaterials with more desirable performance are encouraged to construct biosensors for tyrosinase activity.

Gold/silver nanoclusters (Au/Ag NCs) have attracted widespread attention in recent years. As a bimetallic nanocluster, Au/Ag NCs exhibit its superiority including good stability and excellent biocompatibility and fluorescence performance (Huang et al., 2016). Current studies on Au/Ag NCs are mostly focused on the exploration of synthesis method (Monga and Pal, 2015; Dou et al., 2014; Zhang et al., 2014a), detection of simple ions (Gui and Jin, 2013; Zhang et al., 2014b; Wang et al., 2014) and inorganic substances of interest (Viswanathan et al., 2015), but no research for enzyme assay has been reported to our best knowledge. Herein we propose a convenient and highly sensitive method for tyrosinase activity detection based on dopamine-modified gold/silver nanoclusters. This fluorescent nanoprobe consists of two parts: Au/Ag NCs with strong red luminescence were used as the fluorophore and electron donor, while dopamine with redox property was linked with lipoic acid on the surface of Au/Ag NCs by amide bonds and serves the precursor of *o*-dopaquinone. In the presence of molecular oxygen, dopamine moiety can be readily oxidized into *o*-dopaquinone derivative under the catalysis of tyrosinase. Due to the electron-deficiency property of *o*-dopaquinone, it can serve as the electron acceptor to accept electrons from Au/Ag NCs under irradiation of excitation light. The intraparticle photo-induced election transfer (PET) process could occur between Au/Ag NCs and *o*-dopaquinone moiety in the bioconjugate, which results in fluorescence quenching of the nanoprobe. The correlation between tyrosinase activity and fluorescence signal can be used for quantitative detection of tyrosinase activity.

2. Experimental

2.1. Materials and reagents

Triple-distilled water was used throughout the experimental process. $HAuCl_4 \cdot 3H_2O$, $AgNO_3$, and lipoic acid (LA) were purchased from Sigma-Aldrich company (Shanghai, China). $Na_2HPO_4 \cdot 12H_2O$, $NaH_2PO_4 \cdot 2H_2O$, EDC·HCl, and NHS were purchased from Aladdin Company (Shanghai, China). Tyrosinase (TYR, EC 1.14.18.1) from mushroom, alkaline phosphatase (ALP, EC 3.1.3.1, 10 kU) from bovine intestinal mucosa, bovine serum albumin (BSA), immune globulin G (IgG), acetylcholinesterase (AChE, EC 3.1.1.7), glucose oxidase (GOx, EC 1.1.3.4) and lysozyme (LYS, EC 3.2.1.17) were bought from Sigma-Aldrich (Shanghai, China). Phosphate buffer solution (PB, pH 7.0) was prepared by mixing stock solutions and adjusted to pH 7.0. All reagents were of analytical grade and used without any further purification.

2.2. Synthesis of gold/silver nanoclusters (Au/Ag NCs)

The synthesis of gold/silver nanoclusters was according to our previous paper (Huang et al., 2016). A brief procedure was described as follows: 1.3 mg of lipoic acid was put into 4 mL of NaOH (5 mM) under stirring at room temperature to get a homogeneous solution. Then, 0.208 mL of $HAuCl_4$ (25 mM) and 0.042 mL of $AgNO_3$ (25 mM) at the molar ratio of 5:1 was drop by drop put into the preceding solution under stirring. Afterwards, the solution was heated to 70 °C and kept for 8 h. Finally, the reaction solution was centrifuged at 16,000 rpm for 15 min to discard large particles and dialyzed with water via a dialysis bag (1000 Da) for 48 h to remove the free ions and ligand. As-purified Au/Ag NCs solution was stored at 4 °C for the following experiments.

2.3. Synthesis of dopamine-modified gold/silver nanoclusters (Dopa-Au/Ag NCs) probe

The pH of as-purified Au/Ag NCs solution was adjusted to 5.0. A certain amount of EDC · HCl (0.5 g) and NHS (0.5 g) were added into the Au/Ag NCs solution. The mixture was stirred for 1 h to activate the carboxy groups on the surface of Au/Ag NCs. Then, dopamine (Dopa) (0.5 g) was put into the preceding solution and allowed for 24 h. The pH of the resulting solution was adjusted to 7.0 with NaOH solution (0.5 M), and the resulting solution was bubbled with nitrogen to remove the dissolved oxygen. Finally, as-prepared solution was purified with microporous filter (0.22 μm) and a dialysis bag (1000 Da) to remove excess dopamine, EDC, NHS and possibly generated polydopamine.

2.4. Fluorescent assay of tyrosinase activity

The tyrosinase activity was assessed as extending incubation time with a certain amount of tyrosinase level. The sensing system containing Dopa-Au/Ag NCs (PB, pH 7.0) solution, tyrosinase (796.8 U/L) was monitored by fluorescence spectroscopy every minute. The fluorescence spectra of the system were recorded from 0 to 20 min after the addition of tyrosinase at the excitation wavelength of 319 nm. Under the optimal incubation time (10 min), the activity of tyrosinase was measured. Fluorescence quenching of Dopa-Au/Ag NCs (PB, pH 7.0) was assessed with continuous addition of tyrosinase, where the activity of tyrosinase ranged from 39.9 to 1744.6 U/L. After adding a certain amount of tyrosinase every time, 10 min of incubation time is allowed. The emission spectra of solutions with different amounts of tyrosinase were recorded at an excitation wavelength of 319 nm. The temperature of this experiment was maintained at 37 °C.

2.5. Selectivity test of tyrosinase assay

Under the optimal conditions, the selectivity of the assay toward tyrosinase was conducted as follows. Six possible interferents including immunoglobulin G (lgG), alkaline phosphatase (ALP), acetylcholinesterase (AChE), lysozyme (LYS), bovine serum albumin (BSA), glucose oxidase (GOx) were selected to evaluate the selectivity of the sensing system toward tyrosinase. Dopa-Au/Ag NCs in PB buffer solution (2.5 mL) was first added into the cuvette, and its fluorescence was regarded as the control. Then, each of the following species including lgG, ALP, AChE, LYS, BSA and GOx was separately incubated with Dopa-Au/Ag NCs solution (2.5 mL), where the levels of lgG, ALP, AChE, LYS and TYR are 2000.0 U/L, and the concentrations of BSA and GOx are 0.028 g/L. All the resulting mixtures, which were incubated for 10 min, were monitored using fluorescence spectrophotometer.

2.6. Characterization methods

The morphologies of all samples were characterized by transmission electron microscopy (TEM) The X-ray photoelectron spectroscopy analyses were conducted using a Kratos Axis ULTRA X-ray photoelectron spectrometer. The UV–Vis spectra were recorded on a PerkinElmer Lambda 950 spectrometer. The photoluminescence spectra were conducted on a PerkinElmer LS-55 fluorescence spectrometer, and lifetimes were determined using a FLS 980 fluorescence spectrophotometer.

3. Results and discussion

3.1. Principle of tyrosinase detection based on Dopa-Au/Ag NCs

Gold/silver nanoclusters with the assistance of lipoic acid exhibit its superiority, such as the stable fluorescence emission, wide pH stability, good aqueous solubility, and abundant carboxyl groups from lipoic acid, which makes this nanomaterial a promising candidate for fluorescence reporter (Huang et al., 2016). Dopamine can be used as the functional group due to its redox property (Ma et al., 2015). Under the catalysis of tyrosinase, dopamine can be easily oxidized to *o*-dopaquinone which can serve as a good electron acceptor, and thus dopamine could be the best choice of the functional group. As shown in Scheme 1, the detection strategy of tyrosinase activity is based on intraparticle photoinduced electron transfer process between Au/Ag NCs and *o*-dopaquinone moiety. Dopamine is assembled with Au/Ag NCs by covalent binding with carboxyl group of lipoic acid through EDC/NHS coupling reaction. As-prepared Dopa-Au/Ag NCs nanoprobe emits bright blue fluorescence. In the presence of tyrosinase, dopamine moiety in the nanoprobe can be quickly transformed to *o*-dopaquinone derivative by molecular oxygen because of high catalytic activity of tyrosinase. The electron-deficiency character of generated *o*-dopaquinone derivative enables it as the electron acceptor to accept electrons from Au/Ag NCs under the excitation of light. This intraparticle photoinduced electron transfer process (PET) leads to strong quenching of the fluorescence of Dopa-Au/Ag NCs nanoprobe. The quenched fluorescence is correlated to tyrosinase activity/level involved in the catalytic reaction, which can be used for accurate measurement of tyrosinase activity.

3.2. Synthesis and characterization of Dopa-Au/Ag NCs nanoprobe

The Au/Ag NCs were prepared through the reduction of Au(III) and Ag(I) according to the previous paper (Huang et al., 2016). As-prepared Au/Ag NCs exhibit intense red luminescence, and have a relative narrow size distribution ranging from 2 to 5 nm. XPS spectrum in Fig. S1 displayed dominant signals from oxygen, carbon, sulfur, gold and silver, and the strong signals from oxygen and carbon implies a vast number of oxygen-containing groups including carboxyl on the surface of Au/Ag NCs. Element analysis from XPS spectra indicated that the molar ratio of Au to Ag in Au/Ag NCs is around 6:1, which is close to the molar ratio of starting materials. Dopamine-modified Au/Ag NCs were synthesized using dopamine and Au/Ag NCs through amide formation reaction. Au/Ag NCs abundant in carboxyl group were first activated by EDC/NHS, and then mixed with an excessive amount of dopamine for 24 h at room temperature.

As-prepared Dopa-Au/Ag NCs bioconjugate was purified and characterized by TEM, XPS and fluorescence spectroscopy, respectively. As shown in Fig. 1A, size distribution of Dopa-Au/Ag NCs falls in the range of 2–5 nm, which is consistent with that of Au/Ag NCs because the small dopamine functionalized on the surface of Au/Ag NCs could not apparently change the size of Au/Ag NCs. XPS spectrum in Fig. 1B clearly illustrated that Dopa-Au/Ag NCs are composed of gold, silver, carbon, sulfur, oxygen and nitrogen, and additional nitrogen present in the form of amide (399.17 eV) with respect to pure Au/Ag NCs indicated that dopamine was covalently linked on the surface of Au/Ag NCs through amide bonds. As shown in Fig. 2A, Dopa-Au/Ag NCs has a blue fluorescence at 426 nm, which is an apparent hypsochromic shift by 180 nm compared to that of Au/Ag NCs (608 nm) along with a tremendous blue-shift in optimum excitation peak. This blue-shift in fluorescence of Dopa-Au/Ag NCs with respect to Au/Ag NCs can be attributed to the change of surface ligands induced by the covalent linkage of dopamine to lipoic acid on the surface of Au/Ag NCs (Mishra et al., 2016). Time-resolved fluorescence decay curves of Dopa-Au/Ag NCs conjugate and original Au/Ag NCs were displayed in Fig. S2, and the lifetime of Dopa-Au/Ag NCs conjugate was calculated as 1.66 ns based on the decay curve, which is much shorter than that of Au/Ag NCs (2.88 μs). This large difference in lifetime revealed the modification of dopamine can greatly alter the luminescence performance of Au/Ag NCs. Substantial differences in emission peak and lifetime between Dopa-Au/Ag NCs and original Au/Ag NCs provide further proof for successful preparation of Dopa-Au/Ag NCs.

It has been observed that Au/Ag NCs are stable in various pHs, and its fluorescence remains unchangeable in the pH range of 5.0–9.0. However, we found that dopamine-functionalized Au/Ag NCs conjugate possesses an apparent pH-dependent fluorescence behavior. From Fig. 2B, one can notice that Dopa-Au/Ag NCs probe shows a low fluorescence emission at 410 nm at pH 3–5, and its fluorescence intensity sharply increases when the pH is changed to 7 or 8, which is one of the reasons that pH 7.0 buffer solution was chosen for the following detection. It is surprising that a remarkable bathochromic shift takes place when the pH is turned to 9.0, where the emission peak appears at 500 nm. This obvious change in emission is possibly due to the deprotonation of hydroxyl groups of dopamine moiety of the nanoprobe. This pH-dependent fluorescence change also provides the possibility to establish a pH chemosensor to monitor pH change in local environment in a continuous way. This observation is similar to the finding of dopamine-conjugates (Medintz et al., 2010; Ji et al., 2012), but different in specific changes in terms of intensity or emission color. Stability of Dopa-Au/Ag NCs probe was also assessed when exposed to air as shown in Fig. S3. The fluorescence intensity of Dopa-Au/Ag NCs probe exposed to air gradually decreased to 75% of the original value as a function of time in the range of 0.0–48.0 min, suggesting that the nanoprobe is not very stable in the presence of oxygen. The progressive fluorescence quenching can be attributed to gradual oxidation of dopamine moiety to *o*-dopaquinone by the oxygen molecule in the air. However, the nanoprobe can keep stable for several days under anaerobic condition and at low temperature, and thus the probe

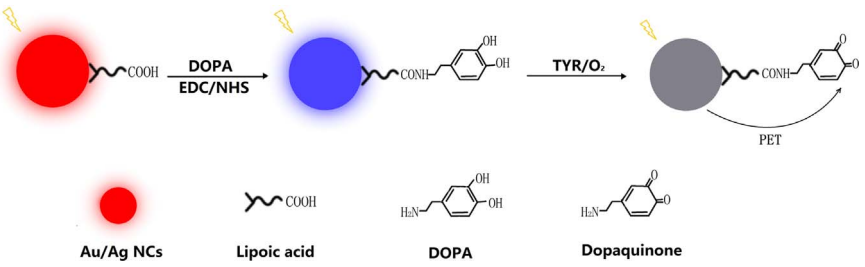

Scheme 1. Detection strategy for TYR activity based on Dopa-Au/Ag NCs bioconjugate through a photoinduced electron transfer process.

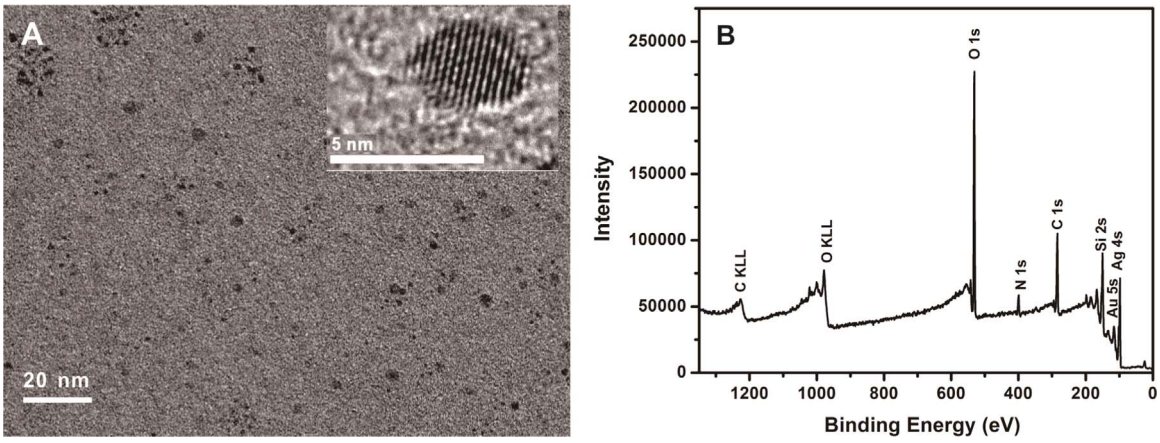

Fig. 1. TEM image (A) and XPS wide spectrum (B) of Dopa-Au/Ag NCs nanoprobe.

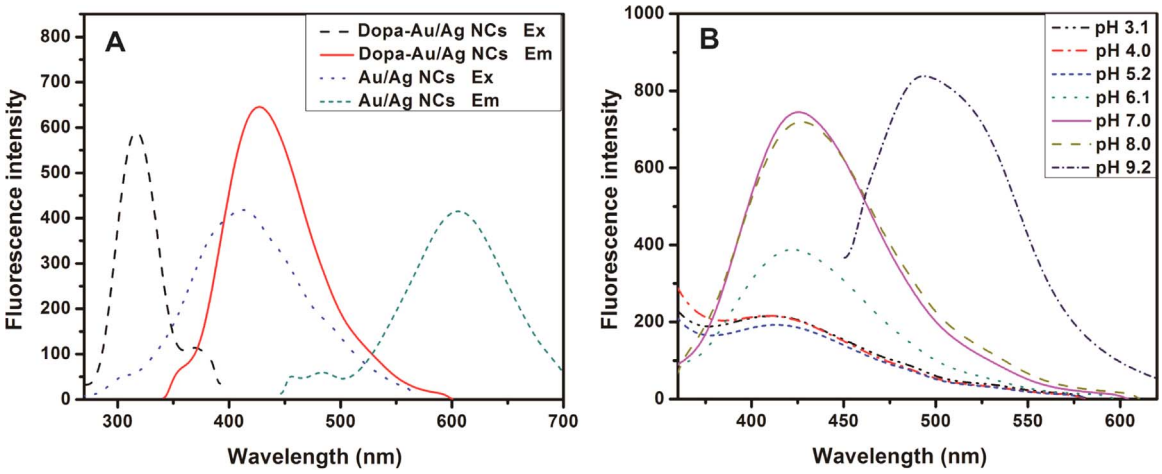

Fig. 2. Fluorescence excitation and emission spectra of Au/Ag NCs and Dopa-Au/Ag NCs (A), and fluorescence spectra of Dopa-Au/Ag NCs at variable pHs (B).

solution must treated with nitrogen molecule to remove oxygen and be stored in the refrigerator.

3.3. *Photoinduced electron transfer process inside Dopa-Au/Ag NCs conjugate under the catalysis of tyrosinase*

An efficient fluorescence quenching was recorded after the introduction of tyrosinase into Dopa-Au/Ag NCs nanoprobe solution as shown in Fig. 3A, where the fluorescence intensity is sharply reduced to 1/8 of the original value after the addition of a high level of tyrosinase (1113.8 U/L) with 10 min of incubation time. It has been proven that dopamine can be rapidly oxidized to *o*-dopaquinone in the presence of molecular oxygen and under the catalysis of tyrosinase. In this case, this transformation of *o*-

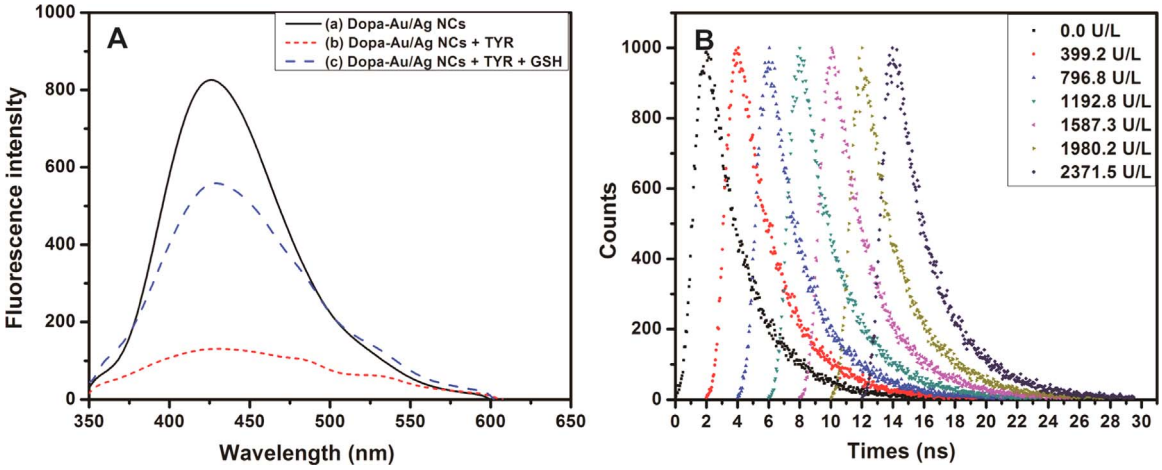

Fig. 3. (A) Changes of fluorescence spectra of Dopa-Au/Ag NCs in the presence of TYR and glutathione (GSH): (a) mere Dopa-Au/Ag NCs, (b) in the presence of TYR (1113.8 U/L), (c) in the presence of TYR (1113.8 U/L) and glutathione (99.8 μM). (B) Normalized time-resolved decay curves of Dopa-Au/Ag NCs nanoprobe in the presence of different amounts of TYR in the rang of 0.0–2371.5 U/L.

dopaquinone from dopamine in the probe possibly contributes to the fluorescence quenching phenomenon. A photoinduced electron transfer process was proposed to explain the nonfluorescent nature of *o*-dopaquinone attached Au/Ag NCs because *o*-dopauinone has been found to be an effective electron acceptor. Thus, the PET process between *o*-dopaquinone and Au/Ag NCs moiety inside the probe leads to the formation of nonfluorescent product. To further verify the underlying nature, glutathione (GSH) was added to reduce *o*-dopaquinone to dopamine derivative because it has been reported that *o*-dopaquinone participates in nucleophilic addition with thiol group of GSH, and *o*-dopaquinone can be turned back to diphenol (Medintz et al., 2010). It is found that fluorescence intensity is recovered after adding a certain amount of GSH. The addition of GSH caused a substantial fluorescence recovery due to the blocking of PET process induced by the reduction of *o*-dopaquinone. Non-fluorescent nature of oxidized product of Dopa-Au/Ag NCs conjugate was also confirmed by time-resolved decay experiment as shown in Fig. 3B. The time-resolved decay curves of Dopa-Au/Ag NCs conjugate in the presence of various amount of tyrosinase were recorded, and the results showed that these decay curves are identical each other, i.e., the lifetimes of luminescent species in the system are the same, which implied that the luminescence is only originated from Dopa-Au/Ag NCs conjugate, and its oxidized product does not fluoresce due to this PET process.

3.4. Real-time fluorescent assay for tyrosinase activity

The fact that the intramolecular photoinduced electron transfer process followed by catalytically oxidation of the nanoprobe in the presence of tyrosinase results in a reduction of fluorescence intensity provides the quantitative correlation between quenched fluorescence and tyrosinase level. Inspired by this correlation, Dopa-Au/Ag NCs nanoprobe has been used to develop fluorometric assay for tyrosinase activity under the optimal detection condition. Phosphate buffer was used in the following experiment because the optimum pH condition of tyrosinase activity is at pH 6-7 (Gauillard et al., 1993; Baron et al., 2005), therefore PB buffer solution (pH 7.0) was chosen as the standard buffer in the following detection. The optimum incubation time for tyrosinase detection was first explored. The fluorescence signal changes of Dopa-Au/Ag NCs conjugate with a certain amount of tyrosinase (796.8 U/L) were recorded at fixed time interval of 1.5 min over a period of 13.2 min. As shown in Fig. 4A, the fluorescence of Dopa-Au/Ag NCs conjugate shows a progressive decline in intensity after the addition of 796.8 U/L of tyrosinase to the solution in a period of 10.0 min. After that, almost unchangeable fluorescence was recorded, indicating that the equilibrium of the oxidation reaction

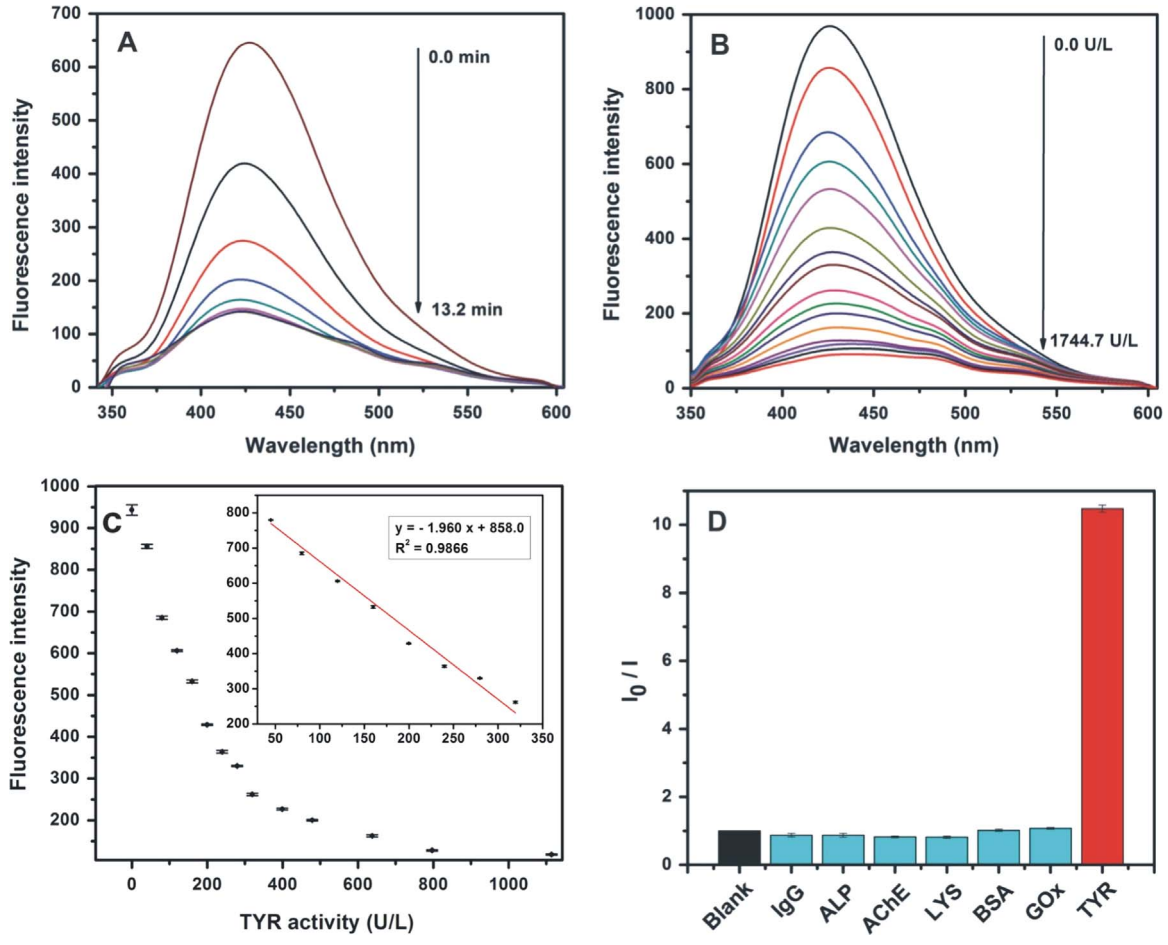

Fig. 4. (A) Fluorescence spectra of Dopa-Au/Ag NCs as a function of reaction time in the presence of tyrosinase (796.8 U/L) at room temperature. Incubation times are 0.0 min, 1.0 min, 3.1 min, 5.1 min, 7.2 min, 9.2 min, 11.2 min and 13.2 min, respectively. (B) Fluorescence spectra of Dopa-Au/Ag NCs as a function of TYR level after 10 min of incubation time. TYR activities/levels are 0.0 U/L, 39.9 U/L, 79.9 U/L, 119.9 U/L, 159.9 U/L, 199.8 U/L, 239.7 U/L, 279.6 U/L, 319.5 U/L, 399.2 U/L, 478.9 U/L, 638.0 U/L, 796.8 U/L, 1113.8 U/L, 1429.7 U/L and 1744.7 U/L, respectively. (C) Fluorescence intensity of Dopa-Au/Ag NCs versus TYR activity ranging from 0.0 to 1744.7 U/L. Inset: The fitting curve and regression equation between fluorescence intensity and TYR activity over a linear range from 45.0 to 319.5 U/L. The relative standard deviation (RSD) for all data varied from 0.3% to 0.9%. (D) Selectivity test of assay toward TYR. I_0 and I represent the fluorescence intensity in the absence and presence of different composition including immunoglobulin G (lg G), alkaline phosphatase (ALP), acetylcholinesterase (AChE), lysozyme (LYS), bovine serum albumin (BSA), glucose oxidase (GOx) and tyrosinase (TYR) separately. The levels of lgG, ALP, AChE, LYS and TYR are 2000.0 U/L, and the concentrations of BSA, GOx are 0.028 g/L.

was attained over 10.0 min

As seen from Fig. 4B, a varying amount of tyrosinase was added into the Dopa-Au/Ag NCs solution under the optimum conditions. The fluorescence of the Dopa-Au/Ag NCs solution with different levels from 0.0 to 1744.7 U/L was recorded after 10 min of incubation time. Within the increasing levels of tyrosinase, the fluorescence of Dopa-Au/Ag NCs conjugate was progressively decreased, and almost completely quenched when tyrosinase level is up to 1744.7 U/L, indicating that most dopamine moiety of the conjugated was catalytically oxidized to *o*-dopaquinone derivatives. Declining trend in fluorescence intensity of Dopa-Au/Ag NCs conjugate was exhibited in Fig. 4C, and there is an excellent linear relationship between fluorescence intensity and tyrosinase activity in the range from 45.0 to 319.5 U/L, which was established as displayed in Fig. 4C inset, and the regression equation can be expressed as $y = -1.960x + 858.0$ with $R^2 = 0.9866$. The detection limit for tyrosinase activity based on three standard errors was calculated to be 13.5 U/L, which is comparable to or slightly better than those based on organic dyes (10–20 U/L) (Yan et al., 2012; Li et al., 2010) and AuNPs (6 U/L) (Teng et al., 2015).

To investigate the possible interference from other enzymes or biospecies toward tyrosinase assay using this method, we evaluated the selectivity of constructed assay for tyrosinase detection in the presence of other possibly interfering species including immunoglobulin G (lg G), alkaline phosphatase (ALP), acetylcholinesterase (AChE), lysozyme (LYS), bovine serum albumin (BSA), glucose oxidase (GOx) separately. As shown in Fig. 4D, the separate addition of GOx, BSA, AChE, ALP and LYS into Dopa-Au/Ag bioconjugate solution results in little influence on the fluorescence in comparison with the blank, however, a sharp decrease in fluorescence intensity was recorded when the same amount of tyrosinase to the others was added in the assay solution. The quenching efficiency was up over 10 while the value of I_0/I for others was around 1 as the blank, which indicates that the proposed Dopa-Au/Ag NCs conjugates exhibit unique discriminative identification for tyrosinase.

4. Conclusion

In general, gold/silver nanoclusters and *o*-dopaquinone were identified as a good electron acceptor and donor pair, and an intraparticle photoinduced electron transfer process between them was used to develop an efficient real-time fluorescent assay for tyrosinase activity based on dopamine-modified gold/silver nanoclusters (Dopa-Au/Ag NCs) nanoprobe. Au/Ag NCs with strong red luminescence were used as the fluorescence reporter, and dopamine with redox property serves as the functional unit in the nanoprobe. In the presence of tyrosinase, dopamine moiety is rapidly oxidized *o*-dopaquinone derivative by molecular oxygen. An efficient photoinduced electron transfer process between Au/Ag NCs and o-dopaquinone derivative induces the following fluorescence quenching. The relationship between tyrosinase activity and fluorescence signal reduction is used to achieve the quantitative evaluation for tyrosinase activity in the range from 45.0 to 319.5 U/L with the detection limit of 13.5 U/L. This study illustrates that gold/silver nanoclusters and *o*-dopaquninone can served as a good electron donor/acceptor pair, and an efficient PET inside this conjugate can occur to cause the change of fluorescence signal. In addition, this Dopa-Au/Ag NCs-based assay provides another way to monitor tyrosinase level, and promise a great potential in medical diagnosis of tyrosinase-associated diseases.

Acknowledgments

We are grateful for the support by the National Natural Science Foundation of China (Nos. 21405142, 21275130 and 21275131).

Appendix A. Supporting information

Supplementary data associated with this article can be found in the online version at doi:10.1016/j.bios.2016.07.051.

References

Baharav, E., Merimski, O., Shoenfeld, Y., Zigelman, R., Gilbrud, B., Yecheskel, G., Youinou, P., Fishman, P., 1996. Clin. Exp. Immunol. 105, 84–88.
Baron, R., Zayats, M., Willner, I., 2005. Anal. Chem. 77, 1566–1571.
D'Andrea, G., D'Amico, D., Bussone, G., Bolner, A., Aguggia, M., Saracco, M.G., Galloni, E., De Riva, V., Colavito, D., Leon, A., Rosteghin, V., Perini, F., 2013. Cephalalgia 33, 932–937.
Dou, X.Y., Yuan, X., Yu, Y., Luo, Z.T., Yao, Q.F., Leong, D.T., Xie, J.P., 2014. Nanoscale 6, 157–161.
Feng, X.L., Feng, F.D., Yu, M.H., He, F., Xu, Q.L., Tang, H.W., Wang, S., Li, Y.L., Zhu, D.B., 2008. Org. Lett. 10, 5369–5372.
Gauillard, F., Richardforget, F., Nicolas, J., 1993. Anal. Biochem. 215, 59–65.
Gui, R.J., Jin, H., 2013. Analyst 138, 7197–7205.
Gill, R., Freeman, R., Xu, J.P., Willner, I., Winograd, S., Shweky, I., Banin, U., 2006. J. Am. Chem. Soc. 128, 15376–15377.
Huang, H., Li, H., Feng, J.J., Wang, A.J., 2016. Sens. Actuators B: Chem. 223, 550–556.
Ji, X., Palui, G., Avellini, T., Na, H.B., Yi, C.Y., Knappenberger, K.L.J., Mattoussi, H., 2012. J. Am. Chem. Soc. 134, 6006–6017.
Kong, F.J., Liu, H.F., Dong, J., Qian, W.P., 2011. Biosens. Bioelectron. 26, 1902–1907.
Li, C., 2006. Colloid. Surf. B 50, 147–151.
Li, S., Mao, L.Y., Tian, Y.P., Wang, J., Zhou, N.D., 2012. Analyst 137, 823–825.
Li, X.H., Shi, W., Chen, S.M., Jia, J., Ma, H.M., Wolfbeis, O.S., 2010. Chem. Commun. 46, 2560–2562.
Lieberman, H.R., Georgelis, J.H., Maher, T.J., Yeghiayan, S.K., 2005. Physiol. Behav. 84, 33–38.
Liu, X.Q., Wang, F.A., Niazov-Elkan, A., Guo, W.W., Willner, I., 2013. Nano Lett. 13, 309–314.
Ma, W., Liu, H.T., Long, Y.T., 2015. ACS Appl. Mater. Interfaces 7, 14352–14358.
Mahoney, C.R., Castellani, J., Kramer, F.M., Young, A., Lieberman, H.R., 2007. Physiol. Behav. 92, 575–582.
Medintz, I.L., Stewart, M.H., Trammell, S.A., Susumu, K., Delehanty, J.B., Mei, B.C., Melinger, J.S., Blanco-Canosa, J.B., Dawson, P.E., Mattoussi, H., 2010. Nat. Mater. 9, 676–684.
Mishra, D., Aldeek, F., Lochner, E., Palui, G., Zeng, B., Mackowski, S., Mattoussi, H., 2016. Langmuir 32, 6445–6458.
Monga, A., Pal, B., 2015. New J. Chem. 39, 304–313.
Park, Y.D., Lee, J.R., Park, K.H., Hahn, H.S., Hahn, M.J., Yang, J.M., 2003. J. Protein Chem. 22, 473–480.
Seo, S.Y., Sharma, V.K., Sharma, N., 2003. J. Agric. Food Chem. 51, 2837–2853.
Sharman, R., Sullivan, K., Young, R.M., McGill, J., 2012. Gene 504, 288–291.
Teng, Y., Jia, X.F., Li, J., Wang, E.K., 2015. Anal. Chem. 87, 4897–4902.
Viswanathan, P., Manivannan, S., Ramaraj, R., 2015. RSC Adv. 5, 54735–54741.
Wang, C.C., Yan, S.Y., Huang, R., Feng, S., Fu, B.S., Weng, X.C., Zhou, X., 2013. Analyst 138, 2825–2828.
Wang, Z.X., Zheng, C.L., Ding, S.N., 2014. RSC Adv. 4, 9825–9829.
Yan, S.Y., Huang, R., Wang, C.C., Zhou, Y.M., Wang, J.Q., Fu, B.S., Weng, X.C., Zhou, X., 2012. Chem. Asian J. 7, 2782–2785.
Yildiz, H.B., Freeman, R., Gill, R., Willner, I., 2008. Anal. Chem. 80, 2811–2816.
Zhang, Y.Y., Jiang, H., Ge, W., Li, Q.W., Wang, X.M., 2014a. Langmuir 30, 10910–10917.
Zhu, X.L., Hu, J., Zhao, Z.H., Sun, M.J., Chi, X.Q., Wang, X.M., Gao, J.H., 2015. Small 11, 862–879.
Zhang, N., Si, Y.M., Sun, Z.Z., Chen, L.J., Li, R., Qiao, Y.C., Wang, H., 2014b. Anal. Chem. 86, 11714–11721.